Capacity Analysis of Index Modulation Multiple Access System

Raed Mesleh, Nareeman Jibreel, and Abdelhamid Younis

***Abstract*—Employing cutting-edge non–orthogonal multiple access (NOMA) techniques, index modulation multiple access (IMMA)introduces an efficient methodology. By leveraging index modulation (IM), IMMA facilitates concurrent data transmission among multiple users. It enhances this process by incorporating an additional constellation diagram that conveys extra information bits per channel utilization. In this work, we conduct a comprehensive investigation. We derive the theoretical capacity of the IMMA system and analyze mutual information across receiver channel estimation scenarios—ranging from perfect to imperfect. To validate our derivations, we execute Monte Carlo simulations, affirming our theoretical results. Notably, our findings confirm that the derived theoretical capacity formula acts as an upper bound for simulated mutual information curves. Additionally, we identify conditions for achieving the derived capacity, rigorously verifying their applicability. Through compelling comparisons, we evaluate the IMMA system's performance in mutual information and capacity against sparse code multiple access (SCMA) systems. This analysis underscores the superior attributes of the IMMA system, showcasing its potential. To illuminate practical constraints, we establish a crucial bound on users effectively sharing orthogonal resources, offering deployment insights. Furthermore, we contrast IMMA systems with traditional orthogonal multiple access (OMA) counterparts, dissecting the implications of overloading. This comprehensive approach yields a holistic comprehension of the scheme's ramifications.**

***Index Terms*—Index modulation (IM), index modulation multiple access (IMMA), multiple–input multiple–output (MIMO), orthogonal frequency division multiple access (OFDMA), sparse code multiple access (SCMA).**

I. Introduction

THE commercialization of 5G marks the culmination of a decade-long journey in wireless communication research. As the world sets its sights on the future, efforts are already underway to shape the landscape of the 6th Generation [1, 2]. These strategic strides have been essential to address the projected 55% annual surge in mobile data traffic over the next decade, aiming to reach a staggering 5000 exabytes by 2030 [3].

In response to this exponential demand for higher spectral efficiency, ultra-low latency, and stringent security requirements, innovative approaches have been introduced [1]. Among these, non-conventional strategies such as non–orthogonal multiple access (NOMA) techniques have emerged. Leveraging NOMA techniques becomes essential as they pave the way to accommodate the burgeoning data traffic, bolstering capacity and connectivity in the upcoming wireless ecosystem [4].

Traditionally, conventional orthogonal multiple access OMA technologies assigned one unique resource to each user. Consequently, the participation of users in a communication process at any given instant hinged upon the availability of orthogonal resources [5]. However, the finite nature of the spectrum necessitated a paradigm shift. Enter the realm of NOMA algorithms, ingeniously enabling co-channel transmission across the limited resources at hand [4]. As we stand at the intersection of technological evolution and unprecedented data demands, NOMA techniques exemplify the audacious strides taken to sculpt the future of wireless communication systems.

In recent years, index modulation (IM) schemes have garnered significant attention for their transformative potential in wireless communication. Leveraging the indices of essential building blocks within communication systems, IM introduces a remarkably efficient digital modulation technique that unlocks the transmission of additional information bits [6–9]. A groundbreaking NOMA innovation, christened index modulation multiple access (IMMA), has emerged as a powerful extension of IM principles [10]. At the core of IM lies an energy- and spectrum-efficient paradigm that holds the promise of revolutionizing future wireless systems. Within the realm of IMMA, the indices of orthogonal resources inherent to corresponding communication systems are ingeniously harnessed to transmit supplementary information bits [11]. This spatial constellation diagram, a testament to innovation, transforms available orthogonal resources (spanning time, frequency, space patterns, and polarization) into a coherent framework. The beauty of this approach lies in its concurrency, eliminating the need for complex scheduling algorithms as all active users gain simultaneous access [10]. The result: the seamless conveyance of extra information bits without physical transmission [11]. This architectural ingenuity becomes evident when comparing the performance of IMMA to the sparse code multiple access (SCMA) scheme, revealing substantial gains [10].

Furthering the innovation trajectory, the concept was iteratively refined in [12] to birth quadrature index modulation multiple access (QIMMA), a correlative sibling of IMMA. In QIMMA, the complex state of the modulated symbol is harnessed to transmit in-phase and quadrature components via separate orthogonal resources. The outcome: A doubling of informational bits conveyed within the spatial domain

Manuscript received April 11, 2023; revised August 27, 2023; approved for publication by Kim, Sang-Hyo, Division 1 Editor, September. 26, 2023.

R. Mesleh is with the Electrical Engineering Department, German Jordanian University, Amman, Jordan, email: raed.mesleh@gju.edu.jo.

R. Mesleh is with the Communication Engineering / IoT Department, Princess Sumaya University for Technology, Amman, Jordan, email: r.mesleh@psut.edu.jo.

N. Jibreel and A. Younis are with the Electrical and Electronics Engineering Department, University of Benghazi, Benghazi, Libya, email: {nariman.alawami, a.alhassi}@uob.edu.ly.

R. Mesleh is the corresponding author.

Digital Object Identifier: 10.23919/JCN.2023.000048

1229-2370/23/$10.00 © 2023 KICS

compared to IMMA.

Building on this foundation, the paper [13] introduced a low-complexity detection method that impressively matches the performance of maximum–likelihood (ML) detection, while dramatically curtailing computational complexity. This innovation further underscores the evolution of IMMA techniques and their tangible impact on the landscape of wireless communication.

While existing literature has predominantly focused on the analysis of average bit error ratio (ABER) performance and the computational intricacies of IMMA and QIMMA systems [12–15], a notable gap persists in addressing the uncharted territory of mutual information and theoretical capacity within the IMMA scheme. This paper endeavors to bridge this gap, yielding a fourfold contribution to the existing body of knowledge:

1) The derivation of mutual information and theoretical capacity bounds for IMMA systems, unveiling critical insights into their information-carrying potential.
2) Unraveling the conditions under which capacity can be achieved, affording a comprehensive understanding across diverse system and channel parameters.
3) A meticulous exploration into the intricate interplay between the number of active users and resultant collision phenomena, shaping the contours of overall system performance.
4) A performance benchmarking exercise, juxtaposing the prowess of IMMA against established systems like SCMA and orthogonal frequency division multiple access (OFDMA).

The subsequent sections of the paper are thoughtfully organized as follows: Section II delves into the intricacies of IMMA and SCMA system models, alongside the accompanying channel models. Section III takes center stage, presenting the analytical derivation of mutual information and theoretical capacity for IMMA systems, followed by thorough discussion. Our findings, coupled with comprehensive discourse, find a home in Section IV. As we approach the conclusion, Section V elegantly ties the threads together, drawing the overarching insights from our endeavors.

II. System Model

A. Index Modulation Multiple Access

Consider an IMMA configuration accommodating N users and L orthogonal resources. Within each discrete time interval, the data stream for every user is compartmentalized into blocks spanning $\log_2 L + \log_2 M$ bits. In the initial $\log_2 L$ segment, a resource index is chosen from the available pool of L resources to facilitate communication. Subsequently, the remaining $\log_2 M$ bits are allocated to modulate a complex symbol drawn from an arbitrary constellation diagram boasting a size M. This modulation occurs exclusively on the selected resource, which becomes active during this interval, facilitating the transmission of the modulated complex symbol, as depicted in Fig. 1.

In the IMMA scheme, data transmission by users occurs simultaneously without the application of any scheduling mechanism. Consequently, collisions arise at the base station

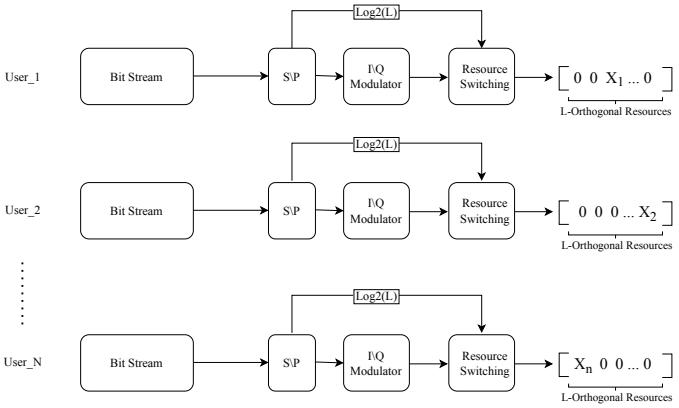

Fig. 1. IMMA system model for N users over L orthogonal resources.

(BS) receiver, causing the reception of signals from all users to be captured in the form [12],

$$\mathbf{y} = \text{diag}(\mathbf{HX}) + \mathbf{n}. \tag{1}$$

Here, $\mathbf{y}$ signifies the L-dimensional received signal, $\mathbf{H}$ represents the $L \times N$ channel matrix depicting the channel gains between each orthogonal resource for each user and the BS receiver, $\mathbf{X}$ stands for the transmitted matrix from all N users across L resource indexes, possessing dimensions $N \times L$, and $\mathbf{n}$ represents the $L-$dimensional additive white Gaussian noise (AWGN) vector, with each element having zero mean and a variance of σ_n^2. The signal received at the ℓth resource index, $\mathbf{y}_l$, is articulated as,

$$\mathbf{y}_l = \sum_{n=1}^{N} h_{nl} x_{nl} + \mathbf{n}_l. \tag{2}$$

Here, h_{nl} signifies the ℓth channel fading gain at the resource index ℓ between the nth user and the BS.

At the receiver end, assuming flawless channel estimation, a joint detection approach is employed for both the signal and the spatial index symbols, facilitated by the ML decoder as follows,

$$[\hat{\mathbf{X}}, \hat{\mathbf{H}}] = \underset{\mathbf{X},\mathbf{H}\in\mathcal{S}}{\arg\min} \left\{ \|\mathbf{y} - \text{diag}(\mathbf{HX})\|_{\text{F}}^2 \right\}, \tag{3}$$

where, $\mathcal{S}$ encompasses the set of all conceivable combinations of users and resource indices.

IMMA Example: For the purpose of illustration, consider the following example. Let the number of users be $N = 3$, and assume a $4-$quadrature amplitude modulation (QAM) constellation diagram ($M = 4$) with $L = 2$ orthogonal frequency resources. The data stream blocks for the three users are as follows: User 1 $\begin{bmatrix}0 & 0 & 1\end{bmatrix}$, User 2 $\begin{bmatrix}0 & 1 & 1\end{bmatrix}$, and User 3 $\begin{bmatrix}1 & 0 & 1\end{bmatrix}$. Within each user's data, the first $\log_2 L = 1$ bit is utilized to select the active resource index, while the subsequent $\log_2 M$ bits modulate a complex symbol from the $4-$QAM constellation diagram. Thus, the transmitted vectors for each user are as follows: $\mathbf{x}_1 = \begin{bmatrix}1+j & 0\end{bmatrix}$, $\mathbf{x}_2 = \begin{bmatrix}1-j & 0\end{bmatrix}$, and $\mathbf{x}_3 = \begin{bmatrix}0 & 1+j\end{bmatrix}$.

The resulting transmitted matrix is formed as:

$$\mathbf{X} = \begin{bmatrix} 1+j & 0 \\ 1-j & 0 \\ 0 & 1+j \end{bmatrix}.$$

It's worth noting that in this example, the first and second users share the first resource, leading to a collision; meanwhile, the third user transmits on the second resource independently.

B. Spare Code Multiple Access

In the context of SCMA, the data bits from each user are partitioned into blocks of $\log_2 M$ bits. These blocks are then mapped to codewords of length L drawn from a unique subset of the SCMA codebook, where each user has an individual codebook [16]. Here, L corresponds to the number of available frequency sub-carriers.

Each user is associated with a constellation matrix $\mathcal{C}_u$ of dimensions $L \times M$, constructed as,

$$\mathcal{C}_u \equiv \mathbf{F}_{L,u} \Delta_u \mathcal{C}_{\mathrm{MC}}, \tag{4}$$

where $\mathbf{F}_{L,u}$ is a factor graph matrix given as

$$\mathbf{F}_{(4,6)} = \begin{bmatrix} 0 & 1 & 1 & 1 & 0 & 0 \\ 1 & 0 & 1 & 0 & 0 & 1 \\ 1 & 0 & 0 & 1 & 1 & 0 \\ 0 & 1 & 0 & 0 & 1 & 1 \end{bmatrix}, \tag{5}$$

and $\mathcal{C}_{\mathrm{MC}}$ denotes the modulation constellation matrix. Designing $\mathcal{C}_{\mathrm{MC}}$ is a crucial step in creating SCMA codebooks [17, 18]. Various techniques exist for designing $\mathcal{C}_{\mathrm{MC}}$. For instance, one approach uses a star-QAM signaling constellation [18], while another utilizes T16-QAM [16]. Additionally, Δ_u represents a constellation operator unique to each user, encompassing operations such as complex conjugation, phase rotation, or dimensional permutation [16, 18].

Table I illustrates the codebook set tailored for six active users across four orthogonal resources. This set comprises complex numbers and serves as the basis for the analysis presented in this paper.

TABLE I
SCMA CODEBOOK SET FOR 6 USERS.

User	Codebook
	00 01 10 11
$\mathcal{C}_1 =$	$\begin{bmatrix} 0 & 0 & 0 & 0 \\ d_{2,1} & d_{2,2} & -d_{2,2} & -d_{2,1} \\ d_{3,1} & d_{3,2} & -d_{3,2} & -d_{3,1} \\ 0 & 0 & 0 & 0 \end{bmatrix}$
$\mathcal{C}_2 =$	$\begin{bmatrix} c_{1,1} & c_{1,2} & -c_{1,2} & -c_{1,1} \\ 0 & 0 & 0 & 0 \\ 0 & 0 & 0 & 0 \\ c_{4,1} & c_{4,2} & -c_{4,2} & -c_{4,1} \end{bmatrix}$
$\mathcal{C}_3 =$	$\begin{bmatrix} a_{1,1} & a_{1,2} & -a_{1,2} & -a_{1,1} \\ a_{2,1} & a_{2,2} & -a_{2,2} & -a_{2,1} \\ 0 & 0 & 0 & 0 \\ 0 & 0 & 0 & 0 \end{bmatrix}$
$\mathcal{C}_4 =$	$\begin{bmatrix} b_{1,1} & b_{1,2} & -b_{1,2} & -b_{1,1} \\ 0 & 0 & 0 & 0 \\ b_{3,1} & b_{3,2} & -b_{3,2} & -b_{3,1} \\ 0 & 0 & 0 & 0 \end{bmatrix}$
$\mathcal{C}_5 =$	$\begin{bmatrix} 0 & 0 & 0 & 0 \\ 0 & 0 & 0 & 0 \\ f_{3,1} & f_{3,2} & -f_{3,2} & -f_{3,1} \\ f_{4,1} & f_{4,2} & -f_{4,2} & -f_{4,1} \end{bmatrix}$
$\mathcal{C}_6 =$	$\begin{bmatrix} 0 & 0 & 0 & 0 \\ e_{2,1} & e_{2,2} & -e_{2,2} & -e_{2,1} \\ 0 & 0 & 0 & 0 \\ e_{4,1} & e_{4,2} & -e_{4,2} & -e_{4,1} \end{bmatrix}$

C. Channel Models

This paper's proposed analysis centers on mutual information and theoretical capacity, with exploration across a variety of channel distributions. For the sake of conciseness, the study narrows down its focus to Rayleigh, Rician, and Nakagami fading channels.

1) Rayleigh Fading: The Rayleigh fading channel involves multiple scattered and reflected paths between the transmitter and receiver, without a direct line-of-sight (LOS) path. This type of fading can be modeled as a zero-mean, unit-variance complex Gaussian random variable [19].

2) Rician Fading: In the Rician channel, transmission paths are composed of a dominant LOS path and additional scattering paths. This channel can be modeled as [19]:

$$\mathbf{H} = \sqrt{\frac{k}{1+k}}\mathbf{H}_{\mathrm{LOS}} + \sqrt{\frac{1}{1+k}}\mathbf{H}_{\mathrm{Ray}}, \tag{6}$$

where $\mathbf{H}_{\mathrm{LOS}}$ and $\mathbf{H}_{\mathrm{Ray}}$ are the LOS matrix and a Rayleigh channel matrix respectively, and k represents the Rician k-factor.

3) Nakagami$-m$ Fading: The Nakagami$-m$ fading channel is a widely used distribution for multi-path modeling in wireless communications. It can be represented as [20],

$$\mathbf{H} = \sqrt{\Omega}\left(sgn(X)\sqrt{\alpha} + jsgn(Y)\sqrt{\beta}\right), \tag{7}$$

where X and Y are modeled as in [20], and α and β are $L \times N$ matrices with entries following a Gamma distribution that has a scale parameter of $1/m$ and a shape parameter of $m/2$.

III. PERFORMANCE ANALYSIS

A. Perfect Channel Knowledge

1) Mutual Information: The mutual information for IMMA system can be defined as the amount of information obtained about the joint index and data symbols, $\mathcal{H}$ and $\mathbf{X}$, by receiving an L length vector $\mathbf{y}$. Let, $\mathcal{H} = \left[\mathbf{h_1}, \mathbf{h_2}, \cdots, \mathbf{h_N}\right]$, where $\mathbf{h_i} = \left[h_l, h_2, \cdots, h_L\right]$, and is assumed to be known perfectly at the receiver. Then,

$$I(\mathbf{X}, \mathcal{H}|\mathbf{Y}) = H(\mathbf{Y}) - H(\mathbf{Y}|\mathbf{X}, \mathcal{H}), \tag{8}$$

where $H(\cdot)$ is the entropy function.

The entropy of $\mathbf{Y}$ is given by,

$$H\left(\mathbf{Y}\right) = -\mathrm{E}_{\mathbf{Y}}\left(\log_2 p_{\mathbf{Y}}\left(\mathbf{y}\right)\right). \tag{9}$$

Then,

$$\begin{aligned} p_{\mathbf{Y}}\left(\mathbf{y}\right) =& \int_{\mathbf{X},\mathcal{H}} p_{\mathbf{x}}\left(\mathbf{X}_i\right) p_{\mathcal{H}}\left(\mathcal{H}_i\right) \times p_{\mathbf{Y}|\mathbf{X},\mathcal{H}}\left(\mathbf{y}|\mathbf{X},\mathcal{H}\right) .d\mathbf{X}_i.d\mathcal{H}_i \\ =& \frac{1}{\left(\pi\sigma_n^2\right)^L} \times \mathrm{E}_{\mathbf{X},\mathcal{H}}\left\{\exp\left(\frac{-\left\|\mathbf{y}-\mathbf{c}\right\|_{\mathrm{F}}^2}{\sigma_n^2}\right)\right\}, \end{aligned} \tag{10}$$

with $\mathbf{c} = \mathrm{diag}(\mathbf{HX})$.

Plugging (10) in (9) yields,

$$\begin{aligned} H\left(\mathbf{Y}\right) =& L\log_2 \pi\sigma_n^2 \\ & -\mathrm{E}_{\mathbf{Y}}\left\{\log_2\left(\mathrm{E}_{\mathbf{X},\mathcal{H}}\left\{\exp\left(\frac{-\left\|\mathbf{y}-\mathbf{c}\right\|_{\mathrm{F}}^2}{\sigma_n^2}\right)\right\}\right)\right\}. \end{aligned} \tag{11}$$

The PDF of $\mathbf{Y}$ knowing $\mathbf{X}$ and $\mathcal{H}$ is a complex Gaussian random vector with mean vector $\mathbf{c}$ and co–variance matrix $\sigma_n^2 \times \mathbf{I}_L$. Hence, $p_{\mathbf{Y}|\mathbf{X},\mathcal{H}}$ is,

$$p_{\mathbf{Y}|\mathbf{X},\mathcal{H}} = \frac{1}{\left(\pi\sigma_n^2\right)^L} \exp\left(\frac{-\left\|\mathbf{y}-\mathbf{c}\right\|_{\mathrm{F}}^2}{\sigma_n^2}\right). \tag{12}$$

The entropy of $\mathbf{Y}$ knowing $\mathbf{X}$ and $\mathcal{H}$ is,

$$\begin{aligned} H\left(\mathbf{Y}|\mathbf{X},\mathcal{H}\right) =& -\mathrm{E}_{\mathbf{Y}|\mathbf{X},\mathcal{H}}\left\{\log_2 p_{\mathbf{Y}|\mathbf{X},\mathcal{H}}\right\} \\ =& L\log_2 \pi\sigma_n^2 \\ & + \log_2\left(\exp\left(1\right)\right)\mathrm{E}_{\mathbf{Y}|\mathbf{X},\mathcal{H}}\left\{\frac{-\left\|\mathbf{y}-\mathbf{c}\right\|_{\mathrm{F}}^2}{\sigma_n^2}\right\} \\ =& L\log_2\left(\pi\sigma_n^2\exp\left(1\right)\right). \end{aligned}$$

Finally, the mutual information can be evaluated as,

$$\begin{aligned} I(\mathbf{X},\mathcal{H}|\mathbf{Y}) =& -L\log_2\left(\exp\left(1\right)\right) \\ & -\mathrm{E}_{\mathbf{Y}}\left\{\log_2\left(\mathrm{E}_{\mathbf{X},\mathcal{H}}\left\{\exp\left(\frac{-\left\|\mathbf{y}-\mathbf{c}\right\|_{\mathrm{F}}^2}{\sigma_n^2}\right)\right\}\right)\right\}. \end{aligned} \tag{13}$$

2) Capacity Analysis: Theoretically, the capacity is defined as the maximum mutual information. In IMMA, the capacity is calculated by maximizing the mutual information joint probability distribution function (PDF) of two symbols, index and signal, as,

$$\begin{aligned} C =& \max_{p_{\mathbf{X}},p_{\mathcal{H}}}\left\{I(\mathbf{X};\mathcal{H}|\mathbf{Y})\right\} \\ =& \max_{p_{\mathbf{X}},p_{\mathcal{H}}}\left\{H(\mathbf{Y})\right\} - H\left(\mathbf{Y}|\mathbf{X},\mathcal{H}_K\right), \end{aligned} \tag{14}$$

where $H\left(\mathbf{Y}|\mathbf{X},\mathcal{H}\right)$ does not depend on either $\mathbf{X}$ or $\mathcal{H}$. Thus, the maximization is performed only over $H(\mathbf{Y})$. The maximization of $H(\mathbf{Y})$ can be achieved if the received vector $\mathbf{Y}$ is complex Gaussian distributed [21], which is realizable if the PDF of $\mathrm{diag}(\mathbf{HX})$ is zero–mean complex Gaussian distribution, *i.e.* $\mathcal{CN}\left(0_L,\mathbf{I}_L\right)$. In this case, the PDF of $\mathbf{Y}$ is,

$$\begin{aligned} p_{\mathbf{Y}}(\mathbf{y}) =& \frac{1}{\pi^L\left|\mathbf{I}_L+\sigma_n^2\mathbf{I}_L\right|}\exp\left(\frac{-\left\|\mathbf{y}\right\|_{\mathrm{F}}^2}{1+\sigma_n^2}\right) \\ =& \frac{1}{\pi^L\left(1+\sigma_n^2\right)^L}\exp\left(\frac{-\left\|\mathbf{y}\right\|_{\mathrm{F}}^2}{1+\sigma_n^2}\right). \end{aligned} \tag{15}$$

Thus, the maximum entropy of $\mathbf{Y}$ is

$$\begin{aligned} H\left(\mathbf{Y}\right) =& L\log_2\left(\pi\left(\sigma_n^2+1\right)\right) \\ & -\log_2(\exp(1)) \times \mathrm{E}_{\mathbf{y}}\left\{\frac{-\left\|\mathbf{y}\right\|_{\mathrm{F}}^2}{1+\sigma_n^2}\right\} \\ =& L\log_2(\pi\left(1+\sigma_n^2\right)) + L\log_2(\exp(1)). \end{aligned} \tag{16}$$

Substituting (16) into (14), a novel capacity formula for IMMA is derived as,

$$C = L\log_2\left(1+\mathrm{SNR}\right). \tag{17}$$

B. Bound on the Number of Users

In IMMA scheme, the bits conveyed every channel use, *i.e.* the word-size is given by,

$$B_t = N \times \log_2 ML. \tag{18}$$

The number of bits conveyed per channel use can not exceed its bound which is the capacity. As such,

$$B_t \leq L\log_2\left(1+\mathrm{SNR}\right), \tag{19}$$

which can also be written as,

$$N \times \log_2 ML \leq L\log_2\left(1+\mathrm{SNR}\right). \tag{20}$$

Therefore,

$$N \leq \frac{L\log_2\left(1+\mathrm{SNR}\right)}{\log_2 ML}. \tag{21}$$

As such, the number of users that can share the same resources is upper bounded by,

$$N \leq \left\lfloor \frac{L\log_2\left(1+\mathrm{SNR}\right)}{\log_2 ML} \right\rfloor, \tag{22}$$

where $\lfloor\rfloor$ being the floor operator.

C. Imperfect Channel Estimation

The consideration of perfect channel knowledge at the receiver is often unattainable due to the stochastic nature of the channel and the influence of AWGN. Consequently, channel estimation techniques are commonly employed to acquire channel information, resulting in imperfect channel estimation. The subsequent sections delve into the effects of channel estimation errors on the theoretical capacity and mutual information within the context of the IMMA scheme.

1) Analysis of Mutual Information: Under the assumption of imperfect channel knowledge, the estimated channel under channel estimation errors (CSE) is given by,

$$\hat{\mathcal{H}} = \mathcal{H} + \mathbf{e}, \tag{23}$$

where $\mathbf{e}$ is an error matrix of size $L \times N$, and each element e_l follows a Gaussian distribution with a mean of zero and a variance of σ_e^2, i.e., $\left(\mathcal{CN}\left(0_N,\sigma_e^2\mathbf{I}_N\right)\right)$.

Consequently, the mutual information under the assumption of imperfect channel knowledge is expressed as follows,

$$I(\mathbf{X},\hat{\mathcal{H}}|\mathbf{Y}) = H\left(\mathbf{Y}\right) - H\left(\mathbf{Y}|\mathbf{X},\hat{\mathcal{H}}\right). \tag{24}$$

The received signal at each resource index is given by,

$$\mathbf{y}_l = \sum_{n=1}^{N} \hat{h}_{nl}\mathbf{x}_{nl} + \mathbf{n}_l. \tag{25}$$

Substituting (23) into (25) yields,

$$\mathbf{y}_l = \sum_{n=1}^{N} h_{nl}\mathbf{x}_{nl} + e_{nl}\mathbf{x}_{nl} + \mathbf{n}_l. \tag{26}$$

Consequently, $\mathbf{c}$ becomes,

$$\mathbf{c} = \mathrm{diag}(\mathbf{HX}) + \mathrm{diag}(\mathbf{eX}). \tag{27}$$

The probability density function (PDF) of $\mathbf{Y}$ given $\mathbf{X}$ and $\mathcal{H}$ is a complex Gaussian random vector with a mean vector $\mathbf{c}$ and a covariance matrix of

$$I_L = \begin{bmatrix} \sigma_n^2 + \sigma_e^2\mathbf{P}_{\mathbf{l}}^{\mathbf{X}} & 0 & 0 & \cdots & 0 \\ 0 & \sigma_n^2 + \sigma_e^2\mathbf{P}_{\mathbf{l}}^{\mathbf{X}} & 0 & \cdots & 0 \\ \vdots & \vdots & \vdots & \ddots & \\ 0 & 0 & 0 & \cdots & \sigma_n^2 + \sigma_e^2\mathbf{P}_{\mathbf{l}}^{\mathbf{X}} \end{bmatrix},$$

where $\mathbf{P}_{\mathbf{l}}^{\mathbf{X}} = \sum_{n\in N} \|\mathbf{x}_{nl}\|_{\mathrm{F}}^2$, and $\sum_{n\in N}$ represents the number of currently active users on the respective orthogonal resource. Let $\Sigma = \bigoplus_{l=1}^{L}(\sigma_n^2 + \sigma_e^2\mathbf{P}_{\mathbf{l}}^{\mathbf{X}})$, where $\bigoplus$ denotes the direct sum [22]. Consequently, the PDF of $\mathbf{Y}$ given $\mathbf{X}$ and $\mathcal{H}$ is formulated as

$$p_{\mathbf{Y}|\mathbf{X},\mathcal{H}} = \frac{1}{\pi^L\Sigma}\exp\left(\frac{-\|\mathbf{y}-\mathbf{c}\|_{\mathrm{F}}^2}{\Sigma}\right). \tag{28}$$

Expressing (28) in (9) results in,

$$H\left(\mathbf{Y}\right) = L\log_2\pi - \mathrm{E}_{\mathbf{Y}}\left\{\log_2\left(\mathrm{E}_{\mathbf{X},\hat{\mathcal{H}}}\left\{\frac{\exp\left(\frac{-\|\mathbf{y}-\mathbf{c}\|_{\mathrm{F}}^2}{\Sigma}\right)}{\Sigma}\right\}\right)\right\}. \tag{29}$$

The entropy of $\mathbf{Y}$ given $\mathbf{X}$ and $\mathcal{H}$ is defined as,

$$H\left(\mathbf{Y}|\mathbf{X},\mathcal{H}\right) = -\mathrm{E}_{\mathbf{X},\mathcal{H}}\left\{\log_2 p_{\mathbf{Y}|\mathbf{X},\mathcal{H}}\right\} \tag{30}$$

$$= L\log_2\pi + \mathrm{E}_{\mathbf{X}}\left\{\log_2\left(\Sigma\right)\right\}. \tag{31}$$

Finally, the mutual information is computed as follows,

$$I(\mathbf{X},\mathcal{H}|\mathbf{Y}) = \mathrm{E}_{\mathbf{X}}\left\{\log_2\left(\Sigma\right)\right\} - \mathrm{E}_{\mathbf{Y}}\left\{\log_2\left(\mathrm{E}_{\mathbf{X},\hat{\mathcal{H}}}\left\{\frac{\exp\left(\frac{-\|\mathbf{y}-\mathbf{c}\|_{\mathrm{F}}^2}{\Sigma}\right)}{\Sigma}\right\}\right)\right\}. \tag{32}$$

2) Capacity Analysis: In the presence of channel imperfections, the capacity is formulated as

$$C = \max_{p_{\mathbf{X}},p_{\hat{\mathcal{H}}}}\left\{I(\mathbf{X};\hat{\mathcal{H}}|\mathbf{Y})\right\} = \max_{p_{\mathbf{X}},p_{\hat{\mathcal{H}}}}\left\{H(\mathbf{Y})\right\} - H\left(\mathbf{Y}|\mathbf{X},\hat{\mathcal{H}}\right), \tag{33}$$

where

$$p_{\mathbf{Y}}(\mathbf{y}) = \frac{1}{\pi^L\left|\mathbf{I}_L + \sigma_n^2\mathbf{I}_L + \sigma_e^2\mathbf{I}_L\right|}\exp\left(\frac{-\|\mathbf{y}\|_{\mathrm{F}}^2}{1+\sigma_n^2+\sigma_e^2}\right) = \frac{1}{\pi^L\left(1+\sigma_n^2+\sigma_e^2\right)^L}\exp\left(\frac{-\|\mathbf{y}\|_{\mathrm{F}}^2}{1+\sigma_n^2+\sigma_e^2}\right). \tag{34}$$

Thus, the maximum entropy of $\mathbf{Y}$ is given by

$$H\left(\mathbf{Y}\right) = L\log_2(\pi\left(1+\sigma_n^2+\sigma_e^2\right)) - \log_2(\exp(1)) \times \mathrm{E}_{\mathbf{y}}\left\{\frac{-\|\mathbf{y}\|_{\mathrm{F}}^2}{1+\sigma_n^2+\sigma_e^2}\right\} = L\log_2(\pi\left(1+\sigma_n^2+\sigma_e^2\right)) + L\log_2(\exp(1)). \tag{35}$$

Substituting (35) into (33), a novel capacity formula for IMMA under imperfect channel estimation is derived as,

$$C = L\log_2(1+\sigma_e^2+\sigma_n^2) - \mathrm{E}_{\mathbf{X}}\left\{\log_2\left(\Sigma\right)\right\}. \tag{36}$$

IV. Results

This section presents the results of Monte Carlo simulations conducted to validate the derived formulas and assess the system's performance under varying conditions. It is essential to emphasize that throughout the presented results, both the channel power σ_h^2 and the transmitted signal power over each resource are normalized and set to 1. Consequently, the signal-to-noise-ratio (SNR) is represented as $1/\sigma_n^2$.

The initial set of results depicted in Fig. 2 serves to confirm the accuracy of the derived formulas, with the derived capacity demonstrated as a true upper bound for all simulated mutual information curves within the IMMA system. The depicted results cover scenarios with 3 or 4 users in the IMMA scheme, as well as using 4-QAM and 8-QAM constellation diagrams. The figure clearly illustrates that both increasing the number of active users and enlarging the constellation diagram size lead to higher achievable mutual information. Additionally, the mutual information curves reach a plateau when the maximum possible spectral efficiency is attained.

A. Achieving the Capacity

In accordance with [21], the attainment of capacity relies on the distribution of $\mathrm{diag}(\mathbf{HX})$ conforming to a zero-mean complex Gaussian distribution, denoted as $\left(\mathcal{CN}\left(0,\sigma^2\right)\right)$.

For example, when the channel distribution follows the Rayleigh model, the optimal distribution of $(\mathbf{X})$ that maximizes conveyed information is the uniform distribution, approximated by a high-order PSK modulation scheme [23, 24]. This observation is verified in Fig. 3, where an IMMA system utilizing a $1024-$PSK constellation, $L = 4$, and $N = 16$, exhibits a joint distribution of $\mathrm{diag}(\mathbf{HX})$ that closely follows a complex Gaussian distribution. Moreover,

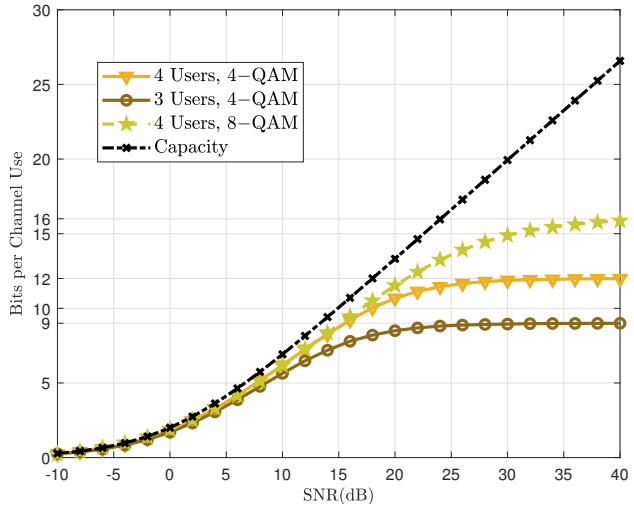

Fig. 2. Mutual information and capacity analysis for IMMA scheme with $L = 2$ orthogonal resources, $N = 3$ and $N = 4$ users, and 4- and 8-QAM constellation diagrams.

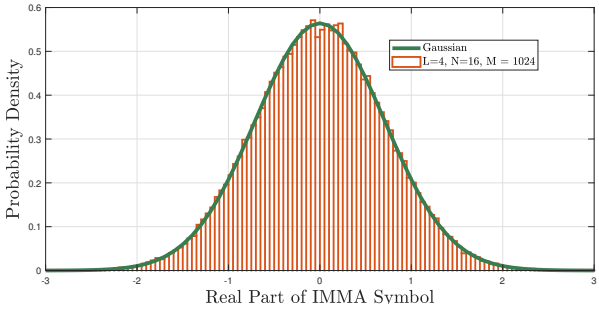

Fig. 3. Histogram of the real part of the index constellation diagram for diag($\mathbf{HX}$) in PSK scheme, compared to the PDF of the Gaussian distribution.

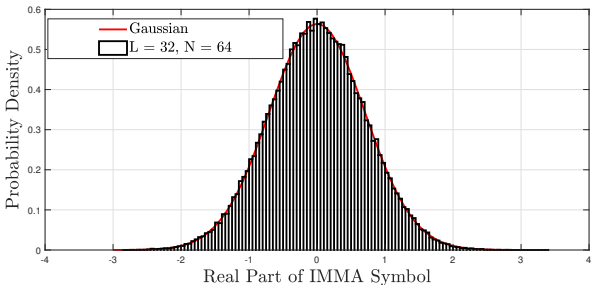

Fig. 4. Histogram of the real part of the index constellation diagram for diag($\mathbf{HX}$), where $M = 0$, compared to the PDF of the Gaussian distribution.

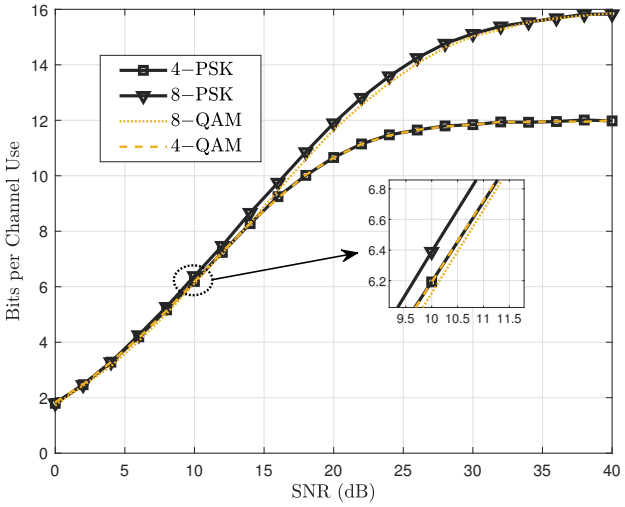

Fig. 5. Mutual information and capacity analysis for the IMMA scheme with QAM and PSK constellation diagrams, considering $M = 4$ and $M = 8$, $L = 2$, and $N = 4$.

in the context of IMMA systems, the capacity emerges as the accumulation of multiple random variables. Interestingly, the theoretical capacity limit can be reached by increasing the count of resources and active users, irrespective of the chosen constellation diagram size. This trend is vividly illustrated in Fig. 4. Although this characteristic underscores a remarkable advantage of the IMMA scheme, it's important to note that deploying an extensive number of users and resources might not be feasible in practical scenarios. Thus, opting for a larger PSK constellation diagram in conjunction with a more modest number of resources and active users can be a pragmatic alternative.

Fig. 5 further corroborates this notion by demonstrating that the IMMA system employing PSK modulation slightly outperforms its counterpart utilizing QAM modulation. This difference in performance can be attributed to the principles discussed earlier.

B. Performance over Variant Fading Channels

The performance evaluation of the IMMA system across Rayleigh, Rician, and Nakagami$-m$ channel distributions is depicted in Fig. 6. The simulation parameters include $L = 2$, $N = 3$, and $M = 8-$QAM, with a Rician channel setting of k = 5 dB and Nakagami$-m$ channel with $m = 5$. The outcomes reveal that the system performs most favorably under Rician fading conditions, while Nakagami$-m$ exhibits the least favorable performance. This discrepancy can be attributed to the pronounced presence of a dominant LOS component in Rician fading, leading to a substantial amplification of the SNR at the receiver. It's worth noting that setting the Rician factor k to 0 effectively transforms the channel into a Rayleigh fading channel. In comparison, the Nakagami$-m$ channel necessitates an additional 2 dB of power to achieve an equivalent level of information conveyance as that of a Rayleigh fading channel.

C. IMMA vs. SCMA Systems

For the purpose of comparison, the SCMA system is also taken into consideration, and the results are depicted in Fig. 7. The previously discussed SCMA system, utilizing the codebook outlined in section II, is employed. This analysis assumes a scenario with $N = 6$ users, $L = 4$ resources, and $M = 4$, resulting in a spectral efficiency of $N \times \log_2(M) = 12$ bits per channel use. The concept of overloading, quantified by the overloading factor denoted as α, pertains to the number of active users relative to the available orthogonal resources. In

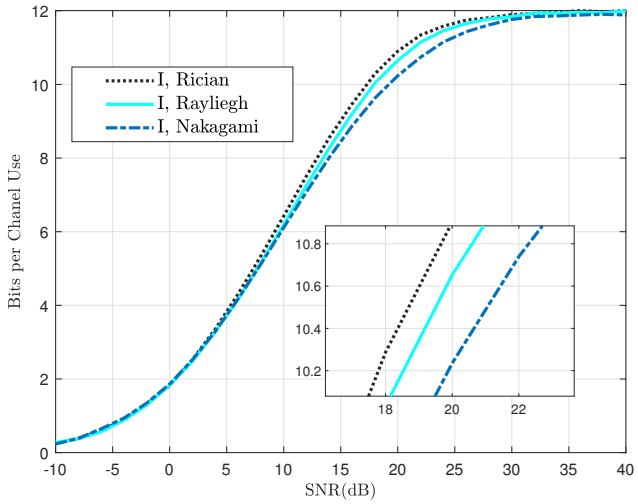

Fig. 6. Exploring the mutual information performance of the IMMA system with $L = 2$, $N = 3$, and $M = 8$-QAM constellation over Rician fading with k = 5 dB, Rayleigh fading, and Nakagami fading.

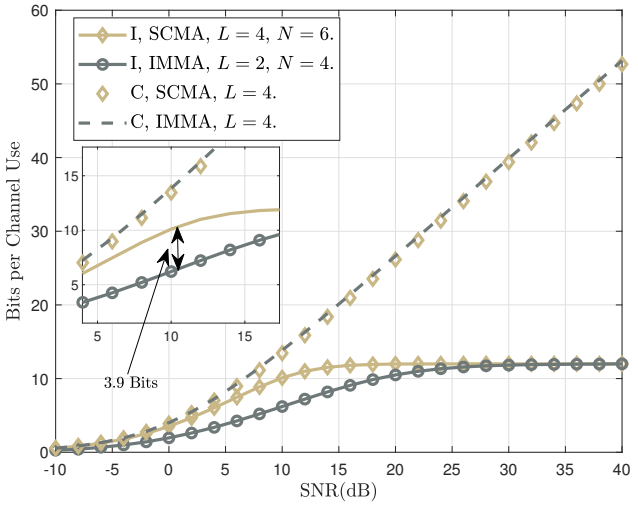

Fig. 7. Comparing IMMA and SCMA systems at 12 bits/s/Hz spectral efficiency.

the context of SCMA, with all users in an active state, α is set at 150% [25, 26].

For reference, the mutual information and capacity of the SCMA scheme have been simulated based on the analytical bounds established in [25]. The ensuing analysis yields the following insights,

$$I\left(\mathbf{X};\mathbf{Y}|\mathbf{H}_1^L\right) = -L\log_2\left(\exp\left(1\right)\right) - \mathrm{E}_{\mathbf{Y}|\mathbf{H}_1^L}\left\{ \log_2\left(\mathrm{E}_{\mathbf{X}}\left\{\exp\left(\frac{-\left\|\sum_{f=1}^{L}\left\|\mathbf{y}_f - \mathbf{H}_f\mathbf{x}_f\right\|_{\mathrm{F}}^2\right\|_{\mathrm{F}}^2}{\sigma_n^2}\right)\right\}\right)\right\}, \tag{37}$$

and

$$C = \mathrm{E}_{\mathbf{H}}\left\{\log_2\left|\bigoplus_{f=1}^{L}\left(\mathbf{I} + \mathrm{SNR}\times\sum_{n_u\in N_f^n}\frac{1}{N}\mathbf{H}_{f,n}\mathbf{H}_{f,n}^H\right)\right|\right\}. \tag{38}$$

The comparison between SCMA and IMMA systems holds particular significance due to their shared attribute of eliminating the necessity for power multiplexing, a feature uncommon in most NOMA schemes. Hence, SCMA systems were deliberately selected for this study's comparative analysis. Despite SCMA systems not necessitating power multiplexing—a complex and intricate procedure—they have their limitations. Notably, they require the pre-allocation of users to available resources and the design of unique codebooks for each user. Comprehensive codebook design details are presented in [25, and references therein]. Additionally, an appropriate set of codebooks that can achieve the theoretical capacity of the system remains to be devised.

In the realm of IMMA systems, the same amount of information, $N \times \log_2(M) = 12$ bits, can be conveyed with the use of $L = 2$ resources, $M = 4$, and $N = 4$, leading to a spectral efficiency of $N \times \log_2(M \times L) = 12$ and an overloading factor $\alpha = 200\%$. This supremacy can be attributed to IMMA systems not employing scheduling techniques, enabling the transmission of more information bits within the frequency slot index used. This differs from SCMA systems where no information is transferred through index modulation. It's important to note that the increased α of the IMMA scheme accounts for its superiority in low SNR conditions. Furthermore, the capacity of the IMMA system with $L = 4$ is marginally higher than that of the SCMA system. Additionally, the theoretical capacity of the IMMA system, as deduced in Section III, remains independent of the channel, setting it apart from SCMA system capacities. Moreover, due to the absence of supplementary diagrams, the capacity of IMMA systems can be effectively realized, as discussed earlier.

D. Bound on Number of Users

At an SNR of 22 dB, employing 2 orthogonal resources with $4-$QAM, the system can effectively accommodate up to 4 users while minimizing information loss. However, as illustrated in Fig. 8, when the number of active users surpasses 4, the occurrence of information loss becomes inevitable. This outcome substantiates the validity of the established limit presented in Section III.

E. Impact of Imperfect Channel Estimation.

The impact of imperfect channel estimation on the capacity of the IMMA system is evident from Fig. 9. This figure demonstrates that systems with imperfect channel knowledge require an additional 2.5 dB of energy to transmit the same number of bits as compared to systems with perfect channel knowledge. A similar trend is observable in the mutual information results, where an extra 3.5 dB of energy is needed to convey an equivalent amount of information under imperfect channel estimation when contrasted with the perfect scenario.

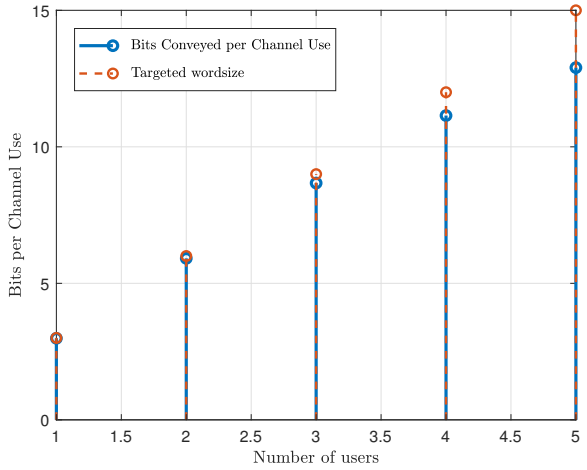

Fig. 8. Comparing conveyed bits and targeted information over a Rayleigh fading channel with 2 orthogonal resources at an SNR of 22 dB.

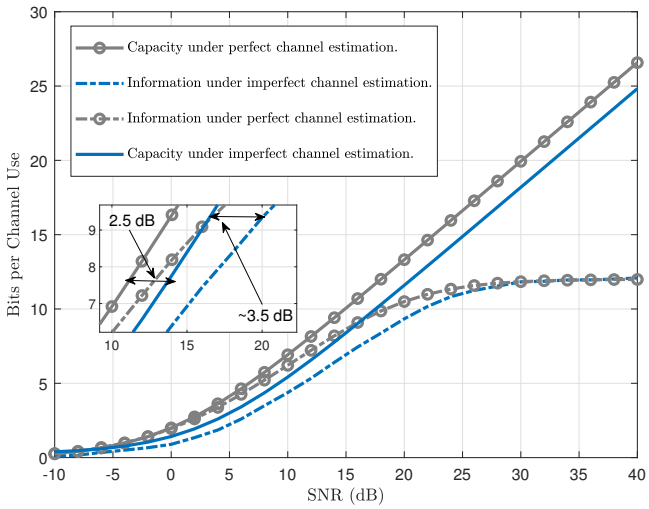

Fig. 9. Mutual information and capacity performance of IMMA system with $M = 4$, $L = 2$, and $N = 4$ under imperfect and perfect channel estimation.

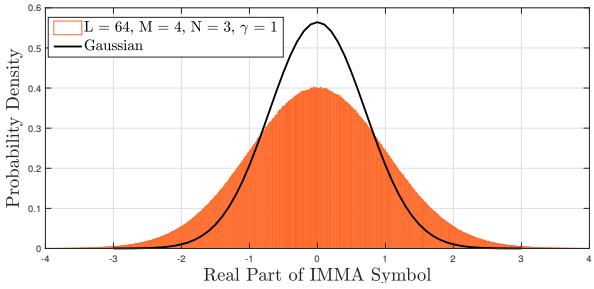

Fig. 10. Histogram of the real part of the index constellation diagram for diag($\mathbf{HX}$) + diag($\mathbf{eX}$), PSK, compared to the PDF of the Gaussian distribution under CSE, with SNR γ = 1.

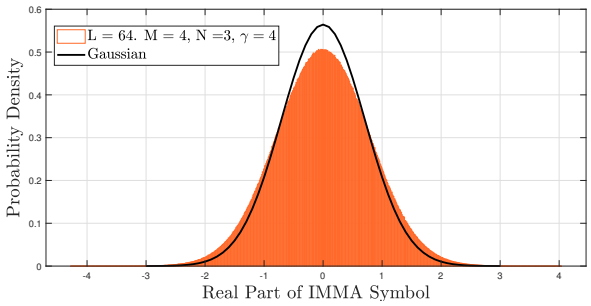

Fig. 11. Histogram of the real part of the index constellation diagram for diag($\mathbf{HX}$) + diag($\mathbf{eX}$), PSK, compared to the PDF of the Gaussian distribution under CSE, with SNR γ = 4.

Furthermore, achieving capacity under the umbrella of CSE becomes challenging when estimation errors are significant, as showcased in Fig. 10. Consider γ as the ratio of channel power to error power, defined by $\gamma = \sigma_h/\sigma_e$. Fig. 10 demonstrates that when $\gamma = 1$, capacity cannot be realized. However, when γ increases—indicating a decrease in the variance of the CSE—the PDF of diag($\mathbf{HX}$) + diag($\mathbf{eX}$) gradually aligns with the Gaussian distribution, as depicted in Fig. 11. This alignment is crucial to achieving the theoretical capacity.

In conclusion, achieving capacity in the presence of CSE hinges on the variance of the CSE, and it becomes feasible with lower σ_e^2 values.

F. Impact of Collision

According to [12], the probability of collision, which is defined as the probability that two or more users occupying the same orthogonal resource, is given by,

$$P_{\text{col}} = \sum_{n=2}^{N} \binom{N}{n} \left(\frac{1}{L}\right)^n \left(1 - \frac{1}{L}\right)^{N-n}. \tag{39}$$

The IMMA scheme confronts collision complexities arising from concurrent user transmissions, wherein collision probability becomes intricately intertwined with both the number of users and the allocation of resources [10, 13]. To delve into a thorough examination of collision probabilities, we kindly guide readers to the source paper, as this manuscript prioritizes brevity and eschews repetitive details. As depicted in Fig. 12, and considering $M = 1$, for all systems, performance degradation can be clearly noticed when the collision probability increases. For instance, when the probability of collision is 0.08, the number of the available resources is twice the number of active users. Hence, it can be stated that a system with low probability of collision, will always outperform a corresponding system experiencing higher chances of collision, which is apparent in the figure. The intricate interplay between collision probability, the targeted word size, and the transmitted bit content is graphically elucidated in Fig.13. As the collision probability escalates, an increasingly conspicuous discrepancy emerges between the initially intended word size and the ultimately transmitted bit content. The graphical representation clearly indicates that elevating the user count inevitably leads to heightened collision probabilities, particularly when the allocation of orthogonal resources remains constant. It is

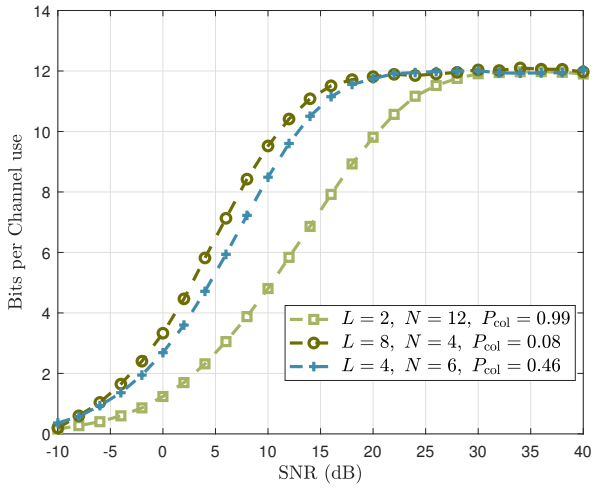

Fig. 12. Impact of collision on IMMA system's performance.

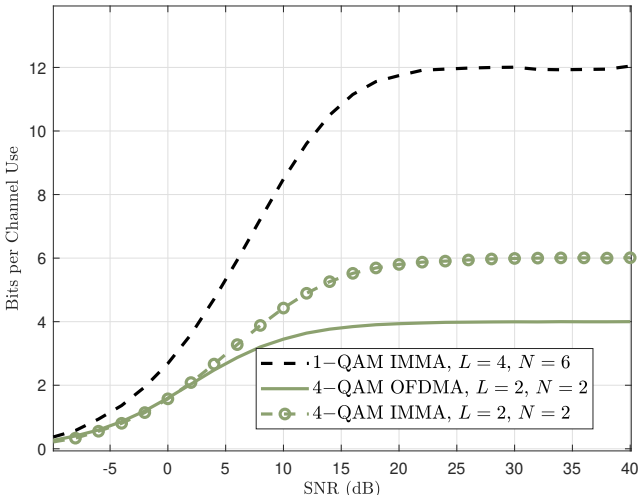

Fig. 14. Comparison between IMMA and OFDMA systems assuming $L = 2$.

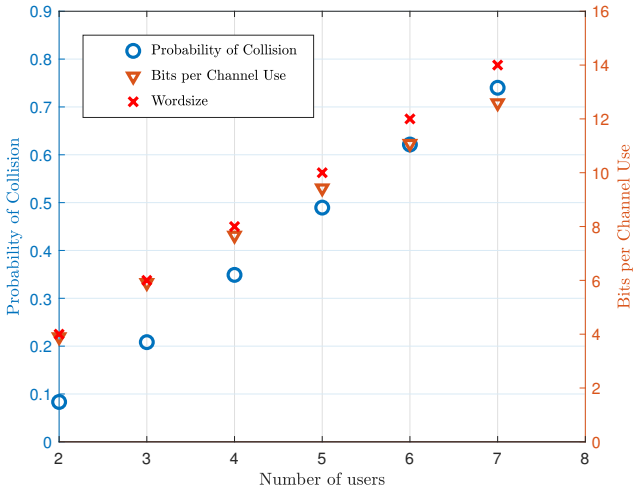

Fig. 13. Bits conveyed per channel use vs. Number of users assigned to 4 orthogonal resources, with $M = 1$, over Rayleigh fading channel, at SNR of $15dB$.

noteworthy that while augmenting the user count significantly enhances the system's overall spectral efficiency, this improvement is coupled with a commensurate increase in collision probability. Consequently, the amplified collision probability poses a considerable challenge to maintaining optimal system performance.

G. OFDMA vs. IMMA

The final set of results depicted in Fig. 14 provides a comparison between the performance of the IMMA system and that of an OFDMA system, with the assumption of $L = 2$, $N = 24$, and $M = 4$−QAM. In the context of the OFDMA system, performance is unaffected by the number of available resources, as it does not involve any IM technique. However, the figure clearly showcases the superiority of the IMMA system, primarily attributed to the utilization of extra bits through IM. One key advantage of the IMMA system is its ability to accommodate more users than the available resources, a feat unattainable in the case of the OFDMA system.

The outcomes presented in Fig. 14 underscore that the IMMA system can be engineered to support up to $N = 6$ users with $L = 4$ resources while exclusively relying on IM and without employing any signal modulation ($M = 1$). Remarkably, this design approach does not result in significant performance degradation, a finding also corroborated by [12].

V. Conclusions

This paper introduces an innovative information theoretical analysis for the IMMA system, unraveling new dimensions of its capabilities. Specifically, we delve into the derivation of both capacity and mutual information metrics for the IMMA system, encompassing scenarios of both perfect and imperfect channel estimation. Notably, our analysis extends to embrace diverse channel fading distributions, including but not limited to Rayleigh, Rice, and Nakagami-m. Within this context, we unveil the conditions that pave the way for achieving the system's capacity, shedding light on their significance through meticulous investigation. Intriguingly, our exploration examines the profound interplay of various system and channel parameters on the overarching performance. Our results underscore that collision occurrences and channel estimation errors wield significant impact on the system's effectiveness, an insight crucial for system designers and implementers. Drawing upon the core tenets of information theory, we unveil an upper bound on the number of active users within the IMMA system—a foundational contribution that shapes the practical deployment landscape. Additionally, our investigation peels back the layers to illustrate the intricate relationship between collision phenomena and the system's capacity and mutual information within the IMMA scheme. This analysis provides a deeper understanding of how such factors intertwine. Comparing our proposed IMMA scheme with existing systems, including SCMA and OFDMA we uncover a noteworthy superiority across diverse performance metrics. This unequivocally positions the IMMA system as

a frontrunner for future system integration, driven by its exceptional attributes. As our research horizons expand, we embark on a journey to comprehensively analyze the fusion of the IMMA system with multiple–input multiple–output (MIMO) techniques. This exploration will peel back the layers of complexity, examining the fusion of additional receiving antennas with orthogonal resources. Through this lens, we anticipate unveiling enhancements in system performance and gaining invaluable insights into the real-world potential of this amalgamation.

REFERENCES

[1] Y.-C. Liang, D. Niyato, E. G. Larsson, and P. Popovski, "Guest editorial: 6G mobile networks: Emerging technologies and applications," *China Commun.*, vol. 17, no. 9, pp. 90–91, 2020.

[2] M. Shafi *et al.*, "5G: A tutorial overview of standards, trials, challenges, deployment, and practice," *IEEE J Sel. Areas Commun.*, vol. 35, no. 6, pp. 1201–1221, 2017.

[3] F. Tariq *et al.*, "A speculative study on 6G," *IEEE Wireless Commun.*, vol. 27, no. 4, pp. 118–125, 2020.

[4] L. Dai *et al.*, "Non-orthogonal multiple access for 5G: Solutions, challenges, opportunities, and future research trends," *IEEE Commun. Mag.*, vol. 53, no. 9, pp. 74–81, 2015.

[5] S. E. El-Khamy, E. E. Sourour, and T. A. Kadous, "Wireless portable communications using pre-RAKE CDMA/TDD/QPSK systems with different combining techniques and imperfect channel estimation," in *Proc. IEEE PIMRC*, 1997.

[6] L. Liang, W. Cheng, W. Zhang, and H. Zhang, "Precoding-based mode hopping for anti-jamming," in *Proc. IEEE GLOBECOM*, 2021.

[7] W. Z. Liping Liang, Wenchi Cheng and H. Zhang, "Index-modulation embedded mode hopping for antijamming," *IEEE Syst. J.*, vol. 16, no. 3, pp. 3905–3916, 2022.

[8] Y. Yang, W. Cheng, W. Zhang, and H. Zhang, "Mode modulation for wireless communications with a twist," *IEEE Trans. Veh. Technol.*, vol. 67, no. 11, pp. 10704–10714, 2018.

[9] E. Basar *et al.*, "Index modulation techniques for next-generation wireless networks," *IEEE Access*, vol. 5, pp. 16693–16746, 2017.

[10] S. Althunibat, R. Mesleh, and T. F. Rahman, "A novel uplink multiple access technique based on index-modulation concept," *IEEE Trans. Commun.*, vol. 67, no. 7, pp. 4848–4855, 2019.

[11] A. A. Raed Mesleh, *Space Modulation Techniques*, 2018.

[12] S. Althunibat, R. Mesleh, and K. Qaraqe, "Quadrature index modulation based multiple access scheme for 5G and beyond," *IEEE Commun. Lett.*, vol. 23, no. 12, pp. 2257–2261, 2019.

[13] J. Li *et al.*, "Low-complexity detection for index modulation multiple access," *IEEE Wireless Commun. Lett.*, vol. 9, no. 7, pp. 943–947, 2020.

[14] W. Belaoura, S. Althunibat, K. Qaraqe, and K. Ghanem, "Precoded index modulation based multiple access scheme," *IEEE Trans. Veh. Technol.*, vol. 69, no. 11, pp. 12912–12920, 2020.

[15] A. Almohamad, S. Althunibat, M. Qaraqe, R. Mesleh, and M. Hasna, "Performance analysis of index modulation based multiple access under imperfect channel estimation," in *Proc. IEEE ComNet*, 2020.

[16] M. Taherzadeh, H. Nikopour, A. Bayesteh, and H. Baligh, "SCMA codebook design," in *Proc. IEEE VTC*, 2014.

[17] M. Alam and Q. Zhang, "Performance study of SCMA codebook design," in *Proc. IEEE WCNC*, 2017.

[18] L. Yu, X. Lei, P. Fan, and D. Chen, "An optimized design of SCMA codebook based on star-QAM signaling constellations," in *Proc. WCSP*, 2015.

[19] M. K. Simon and M. Alouini, *Digital communication over fading channels*, 2nd ed., ser. Wiley series in telecommunications and signal processing. John Wiley & Sons, Inc., 2005, ISBN: 978-0-471-64953-3.

[20] R. Mesleh, O. Badarneh, and A. Younis, "Nakagami-m mimo channel model," in *Proc. ICEEE*, 2022.

[21] C. Shannon, "A mathematical theory of communication," *Bell Syst. Tech. J.*, vol. 27, pp. 379–423 & 623–656, 1948.

[22] D. S. TRACY and R. P. SINGH, "A new matrix product and its applications in partitioned matrix differentiation," *Statistica Neerlandica*, vol. 26, no. 4, 1972.

[23] A. Younis and R. Mesleh, "Information-theoretic treatment of space modulation mimo systems," *IEEE Trans. Veh. Technol.*, vol. 67, no. 8, pp. 6960–6969, 2018.

[24] K. Eltira, N. Jibreel, A. Younis, and R. Mesleh, "Capacity analysis of cooperative amplify and forward multiple–input multiple–output systems," *Trans Emerging Telecommun. Technol.*, vol. 32, 2021.

[25] N. Jibreel, S. Elkawafi, A. Younis, and R. Mesleh, "Performance analysis of sparse code multiple access with variant mimo techniques," *Physical Commun.*, vol. 39, p. 101023, 2020.

[26] N. Jibreel, K. Eltira, A. Younis, and R. Mesleh, "Cooperative amplify and forward ssk sparse code multiple access system: Performance analysis," in *Proc. IEEE MI-STA*, 2021.

Raed Mesleh is currently on sabbatical at Princess Sumaya University for Technology (PSUT) where he serves as the Dean of King Abdullah I School of Graduate Studies and Scientific Research. He is also a Professor in the Communication Engineering / IoT Department at King Abdullah II School of Engineering. He is a Tenured Faculty Member in the Electrical Engineering Department at the German Jordanian University (GJU) and served as the Dean and the Vice Dean of the school of Electrical Engineering and Information Technology for about six years. He received his PhD in 2007 from Jacobs University in Bremen, Germany, and was a Postdoctoral Fellow at Jacobs University from 2007 to 2010. He was with the Electrical Engineering Department at University of Tabuk in Saudi Arabia from 2010 to 2015, where he held the positions of Department Chair and the Director of research excellence and intellectual property units at the deanship of scientific research. He has been a Visiting Scholar at Boston University, The University of Edinburgh, and Herriot-Watt University.

His current research interests include MIMO techniques, terahertz and millimeter wave communications, cell-free systems, physical layer security, Steiner triple systems, graph theory, and optical wireless communication. He is the inventor and co-inventor of 10 patents and has published more than 200 articles in prestigious scientific journals and international conferences. He has an overall citation count of over 13000 with an H-index of 45. He has received Distinguished Researcher Awards from University of Tabuk in 2013 and from GJU in 2016 and 2019. In December 2016, he was honored with the Arab Scientific award from the Arab Thought Foundation.

Nariman Alawami received the B.Sc. degree (Hon.) in Electrical and Electronics Engineering from the University of Benghazi, Libya in 2019. She is currently working for the General Authority for Communication and Informatics. She was an Intern at the Almadar Aljadid R& D center in 2018, and ION telecom and technology company in 2019. Her research interests focus on wireless communication, particularly on MIMO and NOMA techniques.

Abdelhamid Younis is currently on a research visit at the German Jordanian University as part of a research mobility program funded by the Arab-German Young Academy (AGYA) where he has been a member since 2020, and he is an associate professor at the Department of Electrical and Electronics Engineering, University of Benghazi where he joined the department in 2015. He received the B.Sc. (with honors) in 2007 from the University of Benghazi, and the M.Sc. (with distinction) and Ph.D. in 2009 and 2014, respectively, from The University of Edinburgh, U.K. He was the dean of Engineering at the University of Benghazi until 2023 and a Research Associate at the Institute of Digital Communications at the University of Edinburgh from 2013 to 2014. Dr. Younis received the Overseas Research Student Award in 2010, Best Student Paper Award at the 78th IEEE Vehicular Technology Conference (VTC) in Las Vegas, Sep. 2013, the Graphical System Design Achievement Awards Category: Radio Frequency (RF) and Communications from National Instruments (NI) and holds the Almadar Aljadid R&D grant titled "Millimeter-wave large-scale MIMO: ABER and capacity analysis". His main research interests are in the area of wireless communication and digital signal processing with a particular focus on spatial modulation, MIMO wireless communications, and optical wireless communications. He is the Co-author of a book entitle Space Modulation Techniques published by Wiley in 2018.